Stochastic Interval Analysis for Analytical Prediction of the Pattern Tolerance Distribution of a Linear Phased Array with Random Excitation Errors

P. Rocca, N. Anselmi, A. Benoni, and A. Massa

Contents

1 Numerical Results

1.1 Probabilistic IA: Linear Phased Array

1.1.1 Analysis vs Uncertainty Phase Degree

Let us analyse the behaviour of the proposed methodology with $K = 5$ regions, varying the tolerance on the phase shifters, in particular:

- $\xi_n = 1\%,\ n = 1, ..., N$
- $\gamma_n \in [1,\ 10]$ [deg], $n = 1, ..., N$

Test Case Description

Antenna configuration

- isotropic elements
- number of elements: $N = 16$
- distance between elements along x axis: $d_x = \lambda/2$

Nominal excitations

- $W_n = A_n e^{jB_n}$ with $n = 0, .., N-1$
- main lobe steering: broadside
  - $W_n = A_n, B_n = 0\ \forall n$
- Taylor pattern
  - nominal sidelobe level: $SLL_{ref} = -25$ [dB]
  - polinomial order: $\bar{n} = 3$

Excitations tolerances

- Amplitude percentage tolerance: $\xi_n = 1\%$
- Phase tolerance: $\gamma_n \in [1,\ 10]$ [deg]

Probabilistic IA

- hull type: non-convex
- number of sides per polygon: $N_{SIDES} = 720$
- number of pattern regions: $K = 5$

Fig. 1 reports the Probabilistic IA power pattern changing the tolerance on the phases.

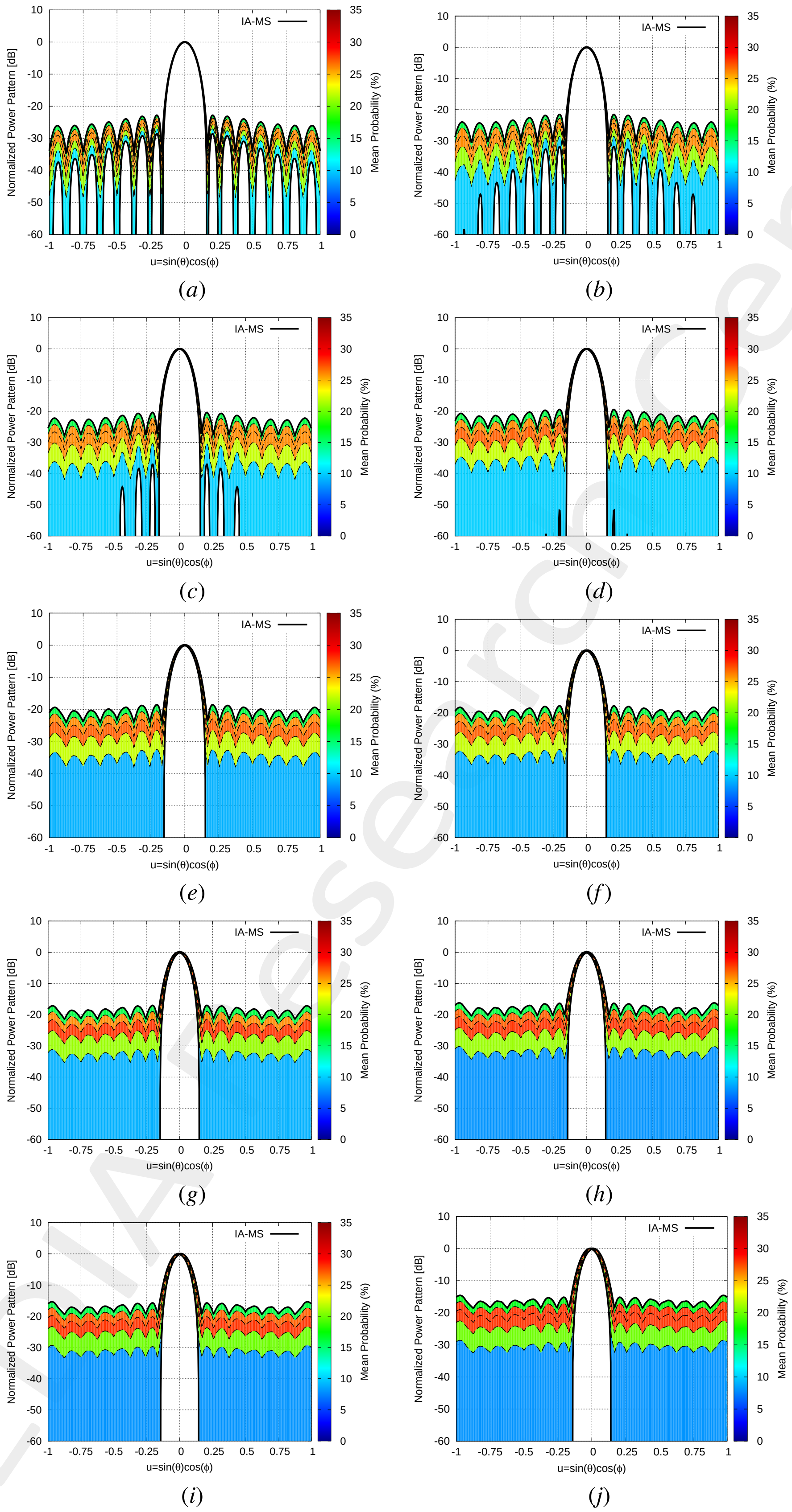

Figure 1: *Probabilistic IA - Linear Array:* (*a*)-(*j*) mean probability of the $K = 5$ regions calculated with the Probabilistic IA method, for $\xi_n = 1\%$and (*a*)$\gamma_n = 1$ [deg] , (*b*) $\gamma_n = 2$ [deg] , (*c*) $\gamma_n = 3$ [deg] , (*d*)$\gamma_n = 4$ [deg] , (*e*) $\gamma_n = 5$ [deg] , (*f*) $\gamma_n = 6$ [deg] , (*g*) $\gamma_n = 7$ [deg] , (*h*)$\gamma_n = 8$ [deg] , (*i*) $\gamma_n = 9$ [deg] and (*j*) $\gamma_n = 10$ [deg].

Power Pattern Features

Fig. 2 shows the variation of the $[SLL]$, $[HPBW]$, $[P_{max}]$ and Δ_n with respect to the tolerance phase $\gamma_n,\ n = 1, ..., N$.

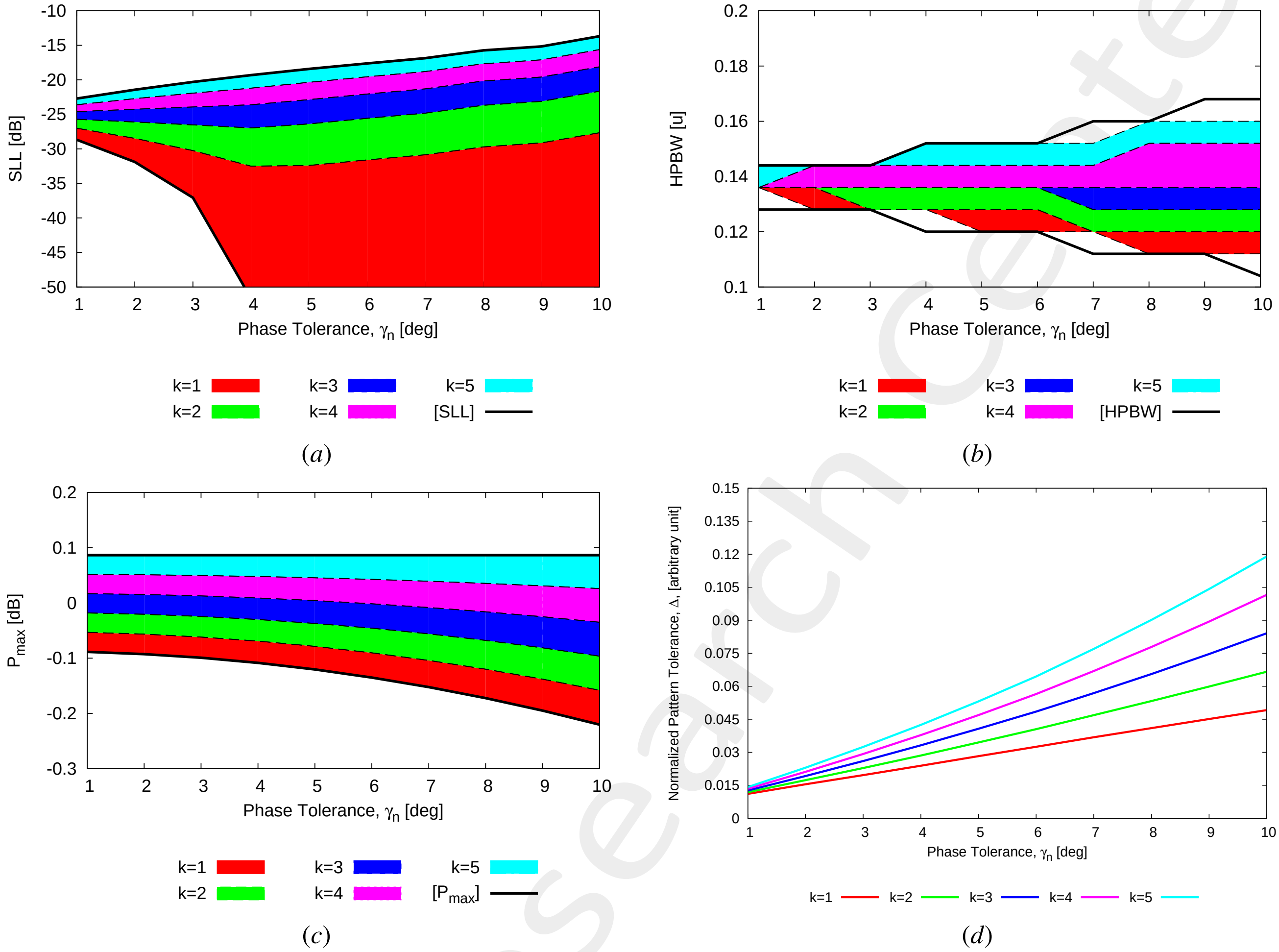

Figure 2: *Performance analysis vs uncertainty phase degree:* behaviour of the power pattern features: (*a*) $[SLL]$ [dB], (*b*) $[HPBW]$ (*c*) $[P_{max}]$ [dB] and (*c*) Δ_n for each of the $K = 5$ regions when setting $\xi_n = 1\%$ and varying the excitation tolerance phases, $\gamma_n \in [1,\ 10]$ [deg].

NOTES:

- For the generation of Fig. 2(a) as lower bound of SLL for each region has been chosen the upper bound of the previous one ($SLL_{k+1}^{inf} = SLL_k^{sup},\ k = 1, ..., K-1$). For the first region has been chosen as lower bound $SLL_1^{inf} = SLL_{IA-MS}^{inf}$.
- For the generation of Fig. 2(b) the upper and lower bounds for $[HPBW]_k$ has been computed only considering $P_{inf}^k(u)$ and $P_{sup}^k(u)$ and not computing $HPBW_k^{worst}$ for $k = 1, ..., K$. In particular, $[HPBW]_k,\ k = 1, ..., K$ has the following expression:

$$[HPBW]_k = [HPBW_k^{inf},\ HPBW_k^{sup}] \quad (1)$$

where $HPBW_k^{inf} = u_{3dB,l}^{inf} - u_{3dB,r}^{inf}$, being $u_{3dB,l}^{inf} = \min\{u :\ P_{inf}^k(u) = P_{inf}^k(u) - 3[\text{dB}]\}$ and $u_{3dB,r}^{inf} = \max\{u :\ P_{inf}^k(u) = P_{inf}^k(u) - 3[\text{dB}]\}$and $HPBW_k^{sup} = u_{3dB,l}^{sup} - u_{3dB,r}^{sup}$, being $u_{3dB,l}^{sup} = \min\{u :\ P_{sup}^k(u) =$

$P^k_{sup}(u) - 3[\text{dB}]\}$ and $u^{sup}_{3dB,r} = \max\{u: \ P^k_{sup}(u) = P^k_{sup}(u) - 3[\text{dB}]\}$.

Tab. I reports the IA-MS power pattern features computed for each $\gamma_n \in [1,\ 10],\ n = 1, ..., N$. Tab. II-XI show the probabilistic power pattern features computed for each $\gamma_n \in [1,\ 10],\ n = 1, ..., N$.

IA-MS				
Phase Tolerance [deg]	$[SLL]$ [dB]	$[HPBW]$ [u]	$[P_{max}]$ [dB]	Δ_n
$\gamma_n = 1$ [deg]	$[-28.678287,\ -22.716413]$	$[0.128,\ 0.144]$	$[-0.088617,\ -0.086508]$	0.063309
$\gamma_n = 2$ [deg]	$[-31.891069,\ -21.431066]$	$[0.128,\ 0.144]$	$[-0.092590,\ 0.086508]$	0.096193
$\gamma_n = 3$ [deg]	$[-37.076208,\ -20.310858]$	$[0.128,\ 0.144]$	$[-0.099206,\ 0.086508]$	0.130241
$\gamma_n = 4$ [deg]	$[-51.635528,\ -19.317522]$	$[0.120,\ 0.152]$	$[-0.108480,\ 0.086508]$	0.165921
$\gamma_n = 5$ [deg]	$[-\infty,\ -18.423585]$	$[0.120,\ 0.152]$	$[-0.120412,\ 0.0865008]$	0.203515
$\gamma_n = 6$ [deg]	$[-\infty,\ -17.618882]$	$[0.120,\ 0.152]$	$[-0.135010,\ 0.086508]$	0.242488
$\gamma_n = 7$ [deg]	$[-\infty,\ -16.867710$	$[0.112,\ 0.160]$	$[-0.152279,\ 0.086508]$	0.284555
$\gamma_n = 8$ [deg]	$[-\infty,\ -15.732658]$	$[0.112,\ 0.160]$	$[-0.172237,\ 0.086508]$	0.327956
$\gamma_n = 9$ [deg]	$[-\infty,\ -15.160057]$	$[0.112,\ 0.168]$	$[-0.194899,\ 0.086508]$	0.373297
$\gamma_n = 10$ [deg]	$[-\infty,\ -13.684748]$	$[0.104,\ 0.168]$	$[-0.220269,\ 0.086508]$	0.420454

Table I: *IA-MS Power Pattern Features:* $[SLL]$, $[HPBW]$, $[P_{max}]$ and Δ_n calculated for the overall interval with $\xi_n = 1\%$ and $\gamma_n \in [1,\ 10]$ [deg].

Phase error: γ_n= 1[deg]				
Region Number	SLL^{worst} [dB]	$HPBW^{worst}$ [u]	$[P_{max}]$ [dB]	Δ_n
$K = 1$	-26.999916	0.144	$[-0.088617,\ -0.053310]$	0.011113
$K = 2$	-25.716782	0.144	$[-0.05331,\ 0.018144]$	0.011887
$K = 3$	-24.597872	0.144	$[-0.18144,\ 0.016883]$	0.012662
$K = 4$	-23.606088	0.144	$[0.016883,\ 0.051767]$	0.013436
$K = 5$	-22.716413	0.136	$[0.051767,\ 0.086508]$	0.014211

Table II: *Probabilistic IA Power Pattern Features:* SLL^{worst}, $HPBW^{worst}$, $[P_{max}]$ and Δ_n for $\xi_n = 1\%$, $\gamma_n = 1$[deg] and $K = 5$ regions.

Phase error: γ_n= 2[deg]				
Region Number	SLL^{worst} [dB]	$HPBW^{worst}$ [u]	$[P_{max}]$ [dB]	Δ_n
$K = 1$	-28.471018	0.144	$[-0.092590,\ -0.056472]$	0.015471
$K = 2$	-26.112542	0.144	$[-0.056472,\ -0.020504]$	0.017354
$K = 3$	-24.257201	0.144	$[-0.020504,\ 0.015312]$	0.019239
$K = 4$	-22.7299873	0.144	$[0.015312,\ 0.050985]$	0.021123
$K = 5$	-21.431066	0.144	$[0.050985,\ 0.086508]$	0.023006

Table III: *Probabilistic IA Power Pattern Features:* SLL^{worst}, $HPBW^{worst}$, $[P_{max}]$ and Δ_n for $\xi_n = 1\%$, $\gamma_n = 2$[deg] and $K = 5$ regions.

Phase error: γ_n= 3[deg]				
Region Number	SLL^{worst} [dB]	$HPBW^{worst}$ [u]	$[P_{max}]$ [dB]	Δ_n
$K = 1$	-30.248777	0.144	$[-0.099206,\ -0.061746]$	0.019643
$K = 2$	-26.526202	0.144	$[-0.061746,\ -0.024441]$	0.022845
$K = 3$	-23.930428	0.144	$[-0.024441,\ 0.012698]$	0.026048
$K = 4$	-21.932970	0.144	$[0.012698,\ 0.049685]$	0.029251
$K = 5$	-20.310858	0.144	$[0.049685,\ 0.086508]$	0.032454

Table IV: *Probabilistic IA Power Pattern Features:* SLL^{worst}, $HPBW^{worst}$, $[P_{max}]$ and Δ_n for $\xi_n = 1\%$, $\gamma_n = 3$[deg] and $K = 5$ regions.

Phase error: γ_n= 4[deg]				
Region Number	SLL^{worst} [dB]	$HPBW^{worst}$ [u]	$[P_{max}]$ [dB]	Δ_n
$K = 1$	-32.495797	0.128	$[-0.108480,\ -0.069131]$	0.023888
$K = 2$	-26.966744	0.128	$[-0.069131,\ -0.029956]$	0.028536
$K = 3$	-23.614790	0.136	$[-0.029956,\ 0.009037]$	0.033184
$K = 4$	-21.203313	0.136	$[0.009037,\ 0.047859]$	0.037832
$K = 5$	-19.3117522	0.144	$[0.047859,\ 0.086508]$	0.042480

Table V: *Probabilistic IA Power Pattern Features:* SLL^{worst}, $HPBW^{worst}$, $[P_{max}]$ and Δ_n for $\xi_n = 1\%$, $\gamma_n = 4$[deg] and $K = 5$ regions.

Phase error: γ_n= 5[deg]				
Region Number	SLL^{worst} [dB]	$HPBW^{worst}$ [u]	$[P_{max}]$ [dB]	Δ_n
$K = 1$	-32.405470	0.152	$[-0.120412,\ -0.078629]$	0.028265
$K = 2$	-26.382928	0.152	$[-0.078629,\ -0.037051]$	0.034485
$K = 3$	-22.860456	0.152	$[-0.037051,\ 0.004332]$	0.040703
$K = 4$	-20.361843	0.152	$[0.004332,\ 0.045518]$	0.046922
$K = 5$	-18.423585	0.152	$[0.045518,\ 0.086508]$	0.053140

Table VI: *Probabilistic IA Power Pattern Features:* SLL^{worst}, $HPBW^{worst}$, $[P_{max}]$ and Δ_n for $\xi_n = 1\%$, $\gamma_n = 5$[deg] and $K = 5$ regions.

Phase error: γ_n= 6[deg]				
Region Number	SLL^{worst} [dB]	$HPBW^{worst}$ [u]	$[P_{max}]$ [dB]	Δ_n
$K = 1$	-31.597765	0.152	$[-0.135010,\ -0.090253]$	0.0322529
$K = 2$	-25.577165	0.152	$[-0.090253,\ -0.045724]$	0.040513
$K = 3$	-22.056059	0.152	$[-0.045724,\ -0.001420]$	0.048498
$K = 4$	-19.55696	0.152	$[-0.001420,\ 0.042655]$	0.056482
$K = 5$	-17.618882	0.152	$[0.042655,\ 0.086508]$	0.064467

Table VII: *Probabilistic IA Power Pattern Features:* SLL^{worst}, $HPBW^{worst}$, $[P_{max}]$ and Δ_n for $\xi_n = 1\%$, $\gamma_n = 6$[deg] and $K = 5$ regions.

Phase error: γ_n= 7[deg]				
Region Number	SLL^{worst} [dB]	$HPBW^{worst}$ [u]	$[P_{max}]$ [dB]	Δ_n
$K = 1$	-30.849516	0.160	$[-0.152279,\ -0.102279]$	0.036829
$K = 2$	-24.82182	0.160	$[-0.103994,\ -0.055975]$	0.046870
$K = 3$	-21.304660	0.160	$[-0.055975,\ -0.008220]$	0.056911
$K = 4$	-18.809524	0.152	$[-0.008220,\ 0.039273]$	0.066951
$K = 5$	-16.867710	0.152	$[0.039273,\ 0.086508]$	0.076993

Table VIII: *Probabilistic IA Power Pattern Features:* SLL^{worst}, $HPBW^{worst}$, $[P_{max}]$ and Δ_n for $\xi_n = 1\%$, $\gamma_n = 7$[deg] and $K = 5$ regions.

Phase error: γ_n= 8[deg]				
Region Number	SLL^{worst} [dB]	$HPBW^{worst}$ [u]	$[P_{max}]$ [dB]	Δ_n
$K = 1$	-29.712058	0.112	$[-0.172237, -0.119867]$	0.041009
$K = 2$	-23.691458	0.120	$[-0.119867, -0.067812]$	0.053301
$K = 3$	-20.169633	0.128	$[-0.067812, -0.016068]$	0.065591
$K = 4$	-17.670858	0.136	$[-0.016068, 0.035372]$	0.077882
$K = 5$	-15.732658	0.152	$[0.035372, 0.086508]$	0.090173

Table IX: *Probabilistic IA Power Pattern Features:* SLL^{worst}, $HPBW^{worst}$, $[P_{max}]$ and Δ_n for $\xi_n = 1\%$, $\gamma_n = 8$[deg] and $K = 5$ regions.

Phase error: γ_n= 9[deg]				
Region Number	SLL^{worst} [dB]	$HPBW^{worst}$ [u]	$[P_{max}]$ [dB]	Δ_n
$K = 1$	-29.138116	0.112	$[-0.194899, -0.137883]$	0.045131
$K = 2$	-23.118447	0.120	$[-0.137883, -0.081239]$	0.059895
$K = 3$	-19.596932	0.128	$[-0.081239, -0.024961]$	0.074659
$K = 4$	-17.098313	0.0136	$[-0.024961, 0.030955]$	0.089423
$K = 5$	-15.160057	0.152	$[0.030955, 0.086508]$	0.104187

Table X: *Probabilistic IA Power Pattern Features:* SLL^{worst}, $HPBW^{worst}$, $[P_{max}]$ and Δ_n for $\xi_n = 1\%$, $\gamma_n = 9$[deg] and $K = 5$ regions.

Phase error: γ_n= 10[deg]				
Region Number	SLL^{worst} [dB]	$HPBW^{worst}$ [u]	$[P_{max}]$ [dB]	Δ_n
$K = 1$	-27.663187	0.168	$[-0.220269, -0.158036]$	0.049184
$K = 2$	-21.643922	0.168	$[-0.158036, -0.096252]$	0.066637
$K = 3$	-18.121652	0.168	$[-0.096252, -0.034905]$	0.084091
$K = 4$	-15.622988	0.160	$[-0.034905, 0.026014]$	0.101544
$K = 5$	-13.684748	0.160	$[0.026014, 0.086508]$	0.118998

Table XI: *Probabilistic IA Power Pattern Features:* SLL^{worst}, $HPBW^{worst}$, $[P_{max}]$ and Δ_n for $\xi_n = 1\%$, $\gamma_n = 10$[deg] and $K = 5$ regions.

Observations:

- Increasing the phase tolerance, the IA-MS bounds become larger. But the two most probable regions are always the third and the fourth ones.
- Analysing the probabilistic power pattern features (Fig. 2 and Tab. II-XI), increasing the phase tolerance the value of the power pattern features increased, too. Moreover, also in this case, the evaluation of $HPBW_k^{worst}$, $k = 1, ..., K$ is difficult because of the sampling adopted.

1.1.2 Analysis vs Number Antenna Elements

Let us analyse the performance of the Probabilistic IA methodology, using different number of antenna elements. In particular, $N = 4,\ 8,\ 16,\ 32$ and 64 has been selected.

Test Case Description

Antenna configuration

- isotropic elements
- number of elements: $N \in \{4,\ 8,\ 16,\ 32,\ 64\}$
- distance between elements along x axis: $d_x = \lambda/2$

Nominal excitations

- $w_n = \alpha_n e^{j\beta_n}$ with $n = 0, .., N-1$
- main lobe steering: broadside
  - $w_n = \alpha_n, \beta_n = 0\ \forall n$
- Taylor pattern
  - nominal sidelobe level: $SLL_{nom} = -25$[dB]
  - polynomial order: $\bar{n} = 3$

Excitations tolerances

- Amplitude percentage tolerance: $\xi_n = 1\%$
- Phase tolerance: $\gamma_n = 3$ [deg]

Probabilistic IA

- hull type: non-convex
- number of sides per polygon: $N_{SIDES} = 720$
- number of pattern regions: $K = 5$

Fig. 3 shows the Probabilistic IA pattern obtained for the different number of antenna elements.

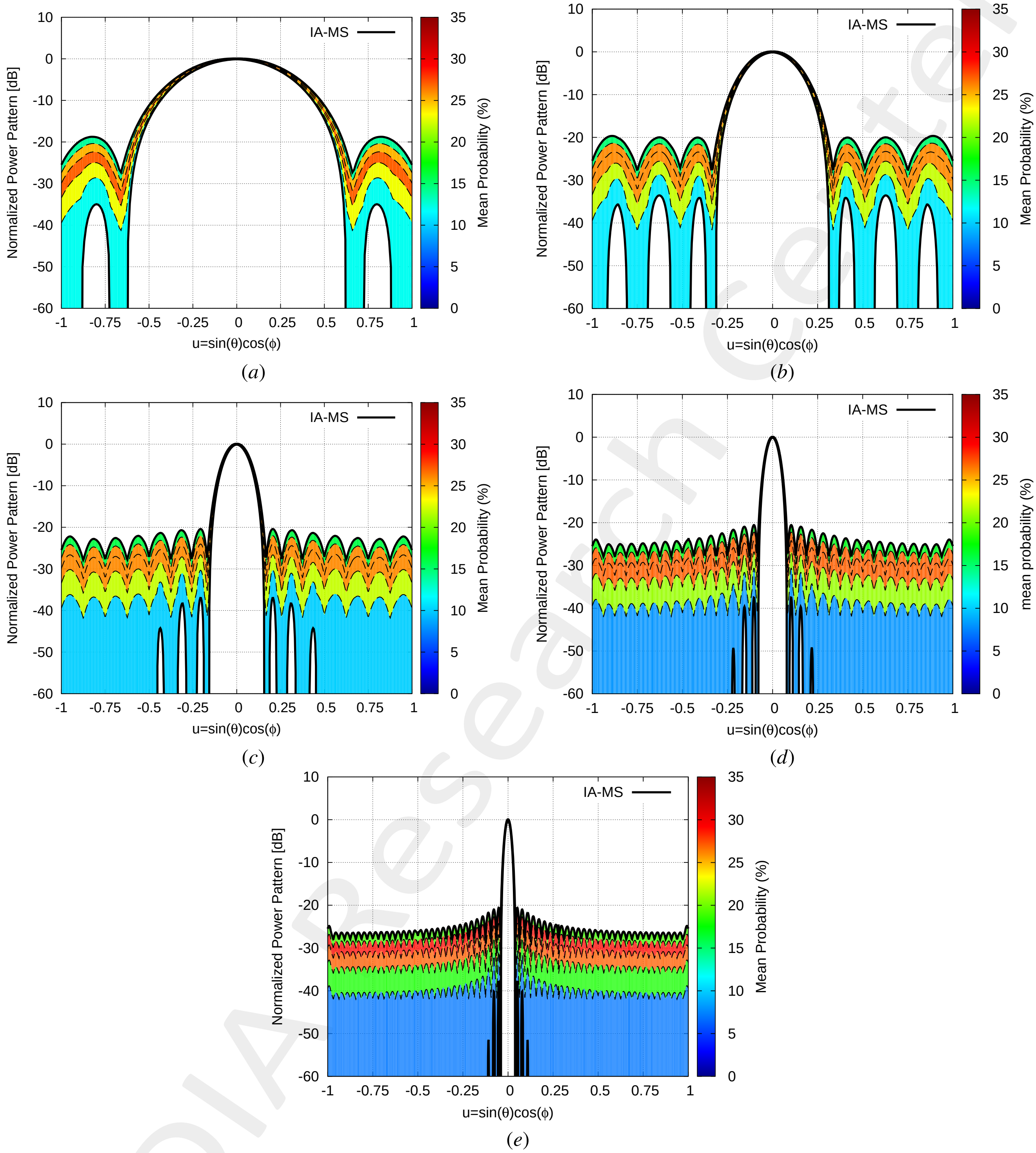

Figure 3: *Probabilistic IA - Analysis vs Number of elements:* mean probability of the $K = 5$ regions calculated with the Probabilistic IA method with excitation tolerances equal to $\xi_n = 1\%$ and $\gamma_n = 3$ [deg], for (*a*) $N = 4$, (*b*) $N = 8$, (*c*) $N = 16$, (*d*) $N = 32$, (*e*) $N = 64$.

Power Pattern Features

Fig. 4 shows the variation of the $[SLL]$, $[HPBW]$, $[P_{max}]$ and Δ_n changing the number of antenna elements.

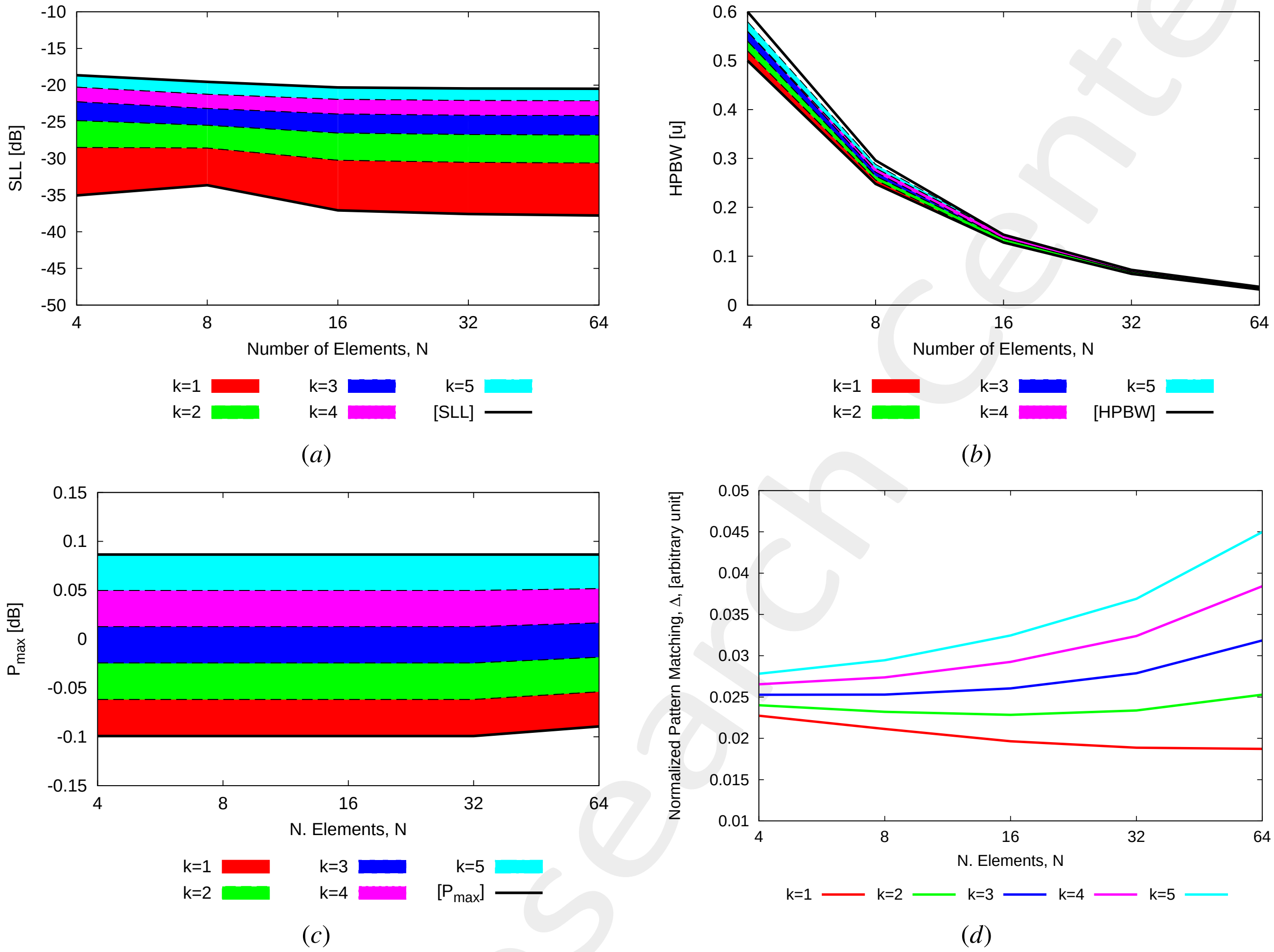

Figure 4: *Performance analysis vs number antenna elements:* behaviour of the power pattern features: (a) $[SLL]$ [dB], (b) $[HPBW]$ (c) $[P_{max}]$ [dB] and (d) Δ_n for each of the $K = 5$ regions when setting $\xi_n = 1\%$ and $\gamma_n = 3$ [deg], varying the number of antenna elements.

Notice that the computation of Fig. 4(a) and (b) has been done according to SubSec. 1.1.

Tab. XII reports the IA-MS power pattern features calculated varying the number of antenna elements. Tab. XIII-XVII shows the probabilistic power pattern features computed considering different number of antenna elements.

IA-MS				
Number Elements	$[SLL]$ [dB]	$[HPBW]$ [u]	$[P_{max}]$ [dB]	Δ_n
$N = 4$	$[-35.048606,\ -18.644026]$	$[0.50,\ 0.60]$	$[-0.099210,\ 0.086513]$	0.126403
$N = 8$	$[-33.651986,\ -19.554505]$	$[0.248,\ 0.296]$	$[-0.099210,\ 0.086513]$	0.126479
$N = 16$	$[-37.076208,\ -20.310858]$	$[0.128,\ 0.144]$	$[-0.099206,\ 0.086508]$	0.130241
$N = 32$	$[-37.582313,\ -20.454976]$	$[0.064,\ 0.072]$	$[-0.099210,\ 0.086513]$	0.139401
$N = 64$	$[-37.782019,\ -20.488108]$	$[0.032,\ 0.037333]$	$[-0.089330,\ 0.086508]$	0.159245

Table XII: *IA-MS Power Pattern Features:* $[SLL]$, $[HPBW]$, $[P_{max}]$ and Δ_n calculated for the overall interval with $\xi_n = 1\%$ and $\gamma_n \in [1,\ 10]$ [deg].

Number of elements: N = 4				
Region Number	SLL^{worst} [dB]	$HPBW^{worst}$ [u]	$[P_{max}]$ [dB]	Δ_n
$K = 1$	-28.508298	0.600	$[-0.099210,\ -0.061746]$	0.022742
$K = 2$	-24.84115	0.600	$[-0.061746,\ -0.02446]$	0.024011
$K = 3$	-22.269506	0.580	$[-0.024446,\ 0.012698]$	0.025281
$K = 4$	-20.271417	0.580	$[0.012698,\ 0.049685]$	0.026550
$K = 5$	-18.644026	0.580	$[0.049685,\ 0.086513]$	0.027820

Table XIII: *Probabilistic IA Power Pattern Features:* SLL^{worst}, $HPBW^{worst}$, $[P_{max}]$ and Δ_n for a $N = 4$ elements linear phased array with $\xi_n = 1\%$, $\gamma_n = 3[\text{deg}]$ and $K = 5$ regions.

Number of elements: N = 8				
Region Number	SLL^{worst} [dB]	$HPBW^{worst}$ [u]	$[P_{max}]$ [dB]	Δ_n
$K = 1$	-28.574992	0.296	$[-0.099210,\ -0.061746]$	0.0214132
$K = 2$	-25.465031	0.288	$[-0.061746,\ -0.024446]$	0.023214
$K = 3$	-23.179811	0.288	$[-0.024446,\ 0.012698]$	0.025296
$K = 4$	-21.244421	0.288	$[0.012698,\ 0.049685]$	0.027378
$K = 5$	-19.554505	0.288	$[0.049685,\ 0.086513]$	0.029460

Table XIV: *Probabilistic IA Power Pattern Features:* SLL^{worst}, $HPBW^{worst}$, $[P_{max}]$ and Δ_n for a $N = 8$ elements linear phased array with $\xi_n = 1\%$, $\gamma_n = 3[\text{deg}]$ and $K = 5$ regions.

Number of elements: N = 16				
Region Number	SLL^{worst} [dB]	$HPBW^{worst}$ [u]	$[P_{max}]$ [dB]	Δ_n
$K = 1$	-30.248777	0.144	$[-0.099206,\ -0.061746]$	0.019643
$K = 2$	-26.526202	0.144	$[-0.061746,\ -0.024441]$	0.022845
$K = 3$	-23.930428	0.144	$[-0.024441,\ 0.012698]$	0.026048
$K = 4$	-21.932970	0.144	$[0.012698,\ 0.049685]$	0.029251
$K = 5$	-20.310858	0.144	$[0.049685,\ 0.086508]$	0.032454

Table XV: *Probabilistic IA Power Pattern Features:* SLL^{worst}, $HPBW^{worst}$, $[P_{max}]$ and Δ_n for a $N = 16$ elements linear phased array with $\xi_n = 1\%$, $\gamma_n = 3[\text{deg}]$ and $K = 5$ regions.

Number of elements: N = 32				
Region Number	SLL^{worst} [dB]	$HPBW^{worst}$ [u]	$[P_{max}]$ [dB]	Δ_n
$K = 1$	-30.525611	0.072	$[-0.099210,\ -0.061746]$	0.018868
$K = 2$	-26.736892	0.072	$[-0.061746,\ -0.02441]$	0.023374
$K = 3$	-24.106384	0.072	$[-0.024441,\ 0.012697]$	0.027880
$K = 4$	-22.089702	0.072	$[0.012698,\ 0.049685]$	0.032386
$K = 5$	-20.454976	0.072	$[0.049685,\ 0.086513]$	0.036892

Table XVI: *Probabilistic IA Power Pattern Features:* SLL^{worst}, $HPBW^{worst}$, $[P_{max}]$ and Δ_n for a $N = 32$ elements linear phased array with $\xi_n = 1\%$, $\gamma_n = 3[\text{deg}]$ and $K = 5$ regions.

Number of elements: $N = 64$				
Region Number	SLL^{worst} [dB]	$HPBW^{worst}$ [u]	$[P_{max}]$ [dB]	Δ_n
$K = 1$	-30.621593	0.037333	$[-0.089330,\ -0.053877]$	0.018725
$K = 2$	-26.799491	0.037333	$[-0.053877,\ -0.018567]$	0.025286
$K = 3$	-24.154173	0.037333	$[-0.018567,\ 0.016602]$	0.031848
$K = 4$	-22.129157	0.037333	$[0.016602,\ 0.051625]$	0.038412
$K = 5$	-20.488108	0.037333	$[0.051625,\ 0.086508]$	0.044974

Table XVII: *Probabilistic IA Power Pattern Features:* SLL^{worst}, $HPBW^{worst}$, $[P_{max}]$ and Δ_n for a $N = 64$ elements linear phased array with $\xi_n = 1\%$, $\gamma_n = 3[\text{deg}]$ and $K = 5$ regions.

Observations:

- As expected, from the analysis conduted until now, from Fig. 3 appears that also in this case the two most probable regions are always the third and fourth ones.
- Analysing the probabilistic power pattern features (Fig. 4 and Tab. XIII-XVII), it is possible to understand that increasing the number of antenna elements, the normalised power pattern matching for each region increases. This behaviour can be explained considering that the number of phasors to be summed together increases. Instead $[P_{max}]_k,\ k = 1, ..., K$ is not influenced by the number of antenna elements. Also in this case $HPBW_k^{worst},\ k = 1, ..., K$ is difficult to be evaluated for each region.

More information on the topics of this document can be found in the following list of references.

References

[1] P. Rocca, N. Anselmi, A. Benoni, and A. Massa, "Probabilistic interval analysis for the analytic prediction of the pattern tolerance distribution in linear phased arrays with random excitation errors," IEEE Trans. Antennas Propag., vol. 68, no. 2, pp. 7866-7878, Dec. 2020.

[2] L. Tenuti, N. Anselmi, P. Rocca, M. Salucci, and A. Massa, "Minkowski sum method for planar arrays sensitivity analysis with uncertain-but-bounded excitation tolerances" IEEE Trans. Antennas Propag., vol. 65, no. 1, pp. 167-177, Jan. 2017.

[3] N. Anselmi, P. Rocca, M. Salucci, and A. Massa, "Optimization of excitation tolerances for robust beamforming in linear arrays," IET Microwaves, Antennas & Propagation, vol. 10, no. 2, pp. 208-214, 2016.

[4] N. Anselmi, P. Rocca, M. Salucci, and A. Massa, "Power pattern sensitivity to calibration errors and mutual coupling in linear arrays through circular interval arithmetics," Sensors, vol. 16, no. 6 (791), pp. 1-14, 2016.

[5] L. Poli, P. Rocca, N. Anselmi, and A. Massa, "Dealing with uncertainties on phase weighting of linear antenna arrays by means of interval-based tolerance analysis," IEEE Trans. Antennas Propag., vol. 63, no. 7, pp. 3299-3234, Jul. 2015.

[6] P. Rocca, N. Anselmi, and A. Massa, "Optimal synthesis of robust array configurations exploiting interval analysis and convex optimization," IEEE Trans. Antennas Propag., vol. 62, no. 7, pp. 3603-3612, July 2014.

[7] T. Moriyama, L. Poli, N. Anselmi, M. Salucci, and P. Rocca, "Real array pattern tolerances from amplitude excitation errors," IEICE Electronics Express, vol. 11, no. 17, pp. 1-8, Sep. 2014.

[8] N. Anselmi, L. Manica, P. Rocca, and A. Massa, "Tolerance analysis of antenna arrays through interval arithmetic," IEEE Trans. Antennas Propag., vol. 61, no. 11, pp. 5496-5507, Nov. 2013.

[9] L. Manica, N. Anselmi, P. Rocca, and A. Massa, "Robust mask-constrained linear array synthesis through an interval-based particle swarm optimisation," IET Microwaves, Antennas and Propagation, vol. 7, no. 12, pp. 976-984, Sep. 2013. P. Rocca, L. Manica, N. Anselmi, and A. Massa, "Analysis of the pattern tolerances in linear arrays with arbitrary amplitude errors," IEEE Antennas Wireless Propag. Lett., vol. 12, pp. 639-642, 2013.

[10] L. Manica, P. Rocca, N. Anselmi, and A. Massa, "On the synthesis of reliable linear arrays through interval arithmetic," IEEE International Symposium on Antennas Propag. (APS/URSI 2013), Orlando, Florida, USA, Jul. 7-12, 2013.

[11] L. Manica, P. Rocca, G. Oliveri, and A. Massa, "Designing radiating systems through interval analysis tools," IEEE International Symposium on Antennas Propag. (APS/URSI 2013), Orlando, Florida, USA, Jul. 7-12, 2013.

[12] M. Carlin, N. Anselmi, L. Manica, P. Rocca, and A. Massa, "Exploiting interval arithmetic for predicting real arrays performances - The linear case," IEEE International Symposium on Antennas Propag. (APS/URSI 2013), Orlando, Florida, USA, Jul. 7-12, 2013.

[13] N. Anselmi, M. Salucci, P. Rocca, and A. Massa, "Generalized sensitivity analysis tool for pattern distortions in reflector antennas with bump-like surface deformations," IET Microwaves, Antennas & Propagation, vol. 10, no. 9, p. 909-916, June 2016.

[14] P. Rocca, L. Poli, N. Anselmi, M. Salucci, and A. Massa, "Predicting antenna pattern degradations in microstrip reflectarrays through interval arithmetic," IET Microwaves, Antennas & Propagation, vol. 10, no. 8, pp. 817-826, May 2016.

[15] P. Rocca, L. Manica, and A. Massa, "Interval-based analysis of pattern distortions in reflector antennas with bump-like surface deformations," IET Microwaves, Antennas and Propagation, vol. 8, no. 15, pp. 1277-1285, Dec. 2014.

[16] P. Rocca, N. Anselmi, and A. Massa, "Interval Arithmetic for pattern tolerance analysis of parabolic reflectors," IEEE Trans. Antennas Propag., vol. 62, no. 10, pp. 4952-4960, Oct. 2014.

[17] P. Rocca, M. Carlin, L. Manica, and A. Massa, "Microwave imaging within the interval analysis framework," Progress in Electromagnetic Research, vol. 143, pp. 675-708, 2013.

[18] L. Manica, P. Rocca, M. Salucci, M. Carlin, and A. Massa, "Scattering data inversion through interval analysis under Rytov approximation," 7th European Conference on Antennas Propag. (EuCAP 2013), Gothenburg, Sweden, Apr. 8-12, 2013.

[19] P. Rocca, M. Carlin, and A. Massa, "Imaging weak scatterers by means of an innovative inverse scattering technique based on the interval analysis," 6th European Conference on Antennas Propag. (EuCAP 2012), Prague, Czech Republic, Mar. 26-30, 2012.

[20] P. Rocca, M. Carlin, G. Oliveri, and A. Massa, "Interval analysis as applied to inverse scattering," IEEE International Symposium on Antennas Propag. (APS/URSI 2013), Chicago, Illinois, USA, Jul. 8-14, 2012.